Physics in Medicine & Biology

PAPER • **OPEN ACCESS**

Direct measurement of ion chamber correction factors, k_Q and k_B, in a 7 MV MRI-linac

To cite this article: Leon de Prez *et al* 2019 *Phys. Med. Biol.* **64** 105025

IOP Publishing Phys. Med. Biol. 64 (2019) 105025 (11pp) https://doi.org/10.1088/1361-6560/ab1511

Physics in Medicine & Biology

IPEM Institute of Physics and Engineering in Medicine

OPEN ACCESS

PAPER

Direct measurement of ion chamber correction factors, k_Q and k_B, in a 7 MV MRI-linac

Leon de Prez[1,2,3], Simon Woodings[2], Jacco de Pooter[1], Bram van Asselen[2], Jochem Wolthaus[2], Bartel Jansen[1] and Bas Raaymakers[2]

[1] VSL—Dutch Metrology Institute, Delft, The Netherlands
[2] Department of Radiotherapy, University Medical Center Utrecht, Utrecht, The Netherlands
[3] Author to whom correspondence may be addressed.

E-mail: ldprez@vsl.nl

RECEIVED
15 February 2019

REVISED
20 March 2019

ACCEPTED FOR PUBLICATION
1 April 2019

PUBLISHED
21 May 2019

Keywords: absorbed dose, magnetic field, k_Q, k_B, MRgRT

Abstract

The output of MRI-integrated photon therapy (MRgXT) devices is measured in terms of absorbed dose to water, D_w. Traditionally this is done with reference type ion chambers calibrated in a beam quality Q_0 without magnetic field. To correct the ion chamber response for the application in the magnetic field, a factor needs to be applied that corrects for both beam quality Q and the presence of the magnetic field B, $k_{Q,B}$. This can be expressed as the product of k_Q, without magnetic field, and ion chamber magnetic field correction, k_B. k_B depends on the magnetic field strength and its direction, the direction of the beam and the orientation and type of the ion chamber. In this study, for the first time, both k_Q and k_B were measured directly for six waterproof ion chambers (3 $\times$ PTW 30013 and 3 $\times$ IBA FC65-G) in a pre-clinical 7 MV MRI-linac at 0 T and at 1.5 T. Measurements were done with the only available primary standard built for this purpose, a water calorimeter. Resulting k_Q factors for PTW and IBA chambers were 0.985(5) and 0.990(4), respectively. k_B factors were measured with the chambers in antiparallel direction to the magnetic field ($\parallel$ 180°), and perpendicular direction ($\perp$ −90°). $k_{B\parallel}$ and $k_{B\perp}$ for the PTW chambers were 0.985(6) and 0.963(4), respectively and for IBA chambers 0.995(4) and 0.956(4). Agreement with the available literature values was shown, partly caused by the relatively large standard deviation (SD) in those values. The values in this study are currently the only available measured values for k_Q and k_B in an MRI-linac that are directly linked to the international traceability framework for the quantity absorbed dose to water, D_w.

1. Introduction

MRI guided radiotherapy (MRgRT) uses an MRI scanner integrated with a treatment machine and allows for unprecedented real-time visualization and motion tracking of the target during the actual treatment, in real time. Several, integrated MRgRT devices are under development or in clinical use (Fallone 2014, Keall *et al* 2014, Mutic and Dempsey 2014, Raaymakers *et al* 2017). However, dosimetry in the presence of a magnetic field, B, is not trivial. The energy deposition of the secondary electrons trajectories is influenced by the Lorentz force and dose distributions change e.g. in build-up and penumbra regions, with depth and in regions with material and density inhomogeneities (Raaymakers *et al* 2004, Raaijmakers *et al* 2008, Oborn *et al* 2010, Woodings *et al* 2018). Traditionally, photon beams in radiotherapy are calibrated in terms of absorbed dose to water, D_w, by ion chambers calibrated in beam quality Q_0 (usually ^{60}Co), $N_{D_w Q_0}$, without magnetic field (Andreo *et al* 2000, Aalbers *et al* 2008, McEwen *et al* 2014). The most fundamental and direct method to calibrate detectors for reference dosimetry is against a primary standard[3] that realizes the unit Gray (Gy) for D_w, at the reference point in a water phantom. The ion chamber calibration coefficients, N_{D_w}, is established by dividing D_w by the ion chamber reading, M, corrected for influence quantities (Almond *et al* 1999, Andreo *et al* 2000):

[3] A primary standard is defined as a measurement standard obtaining a measurement result without relation to a measurement standard for a quantity of the same kind (OIML 2007).

$$N_{D_w} = \frac{D_w}{M}. \quad (1)$$

Reference dosimetry in MRI-integrated photon therapy (MRgXT) devices is done with ion chambers that are placed in the magnetic field of an MRI-linac. Therefore, the change in ion chamber response needs to be corrected for both beam quality, Q, and magnetic field, B, by a factor $k_{Q,B}$. D_w is determined according to:

$$D_w = k_{Q,B} \cdot M \cdot N_{D_w Q_0}. \quad (2)$$

The correction factor $k_{Q,B}$ is, in analogy to k_Q (Andreo 1992), defined as the ratio between its calibration coefficients in beam quality Q with magnetic field, $N_{D_w,Q,B}$, and that in reference beam quality Q_0 without magnetic field, N_{D_w,Q_0}:

$$k_{Q,B} = \frac{N_{D_w,Q,B}}{N_{D_w,Q_0}}. \quad (3)$$

Another approach is to apply the product of two independent correction factors, i.e. a beam quality correction for the MRI-linac photon beam without magnetic field, k_Q, and a magnetic field correction k_B:

$$k_{Q,B} = k_Q \cdot k_B = \frac{N_{D_w,Q}}{N_{D_w,Q_0}} \cdot \frac{N_{D_w,Q,B}}{N_{D_w,Q}}. \quad (4)$$

Monte Carlo calculations and measurements showed that the magnetic field affects k_B by several percent (Meijsing *et al* 2009, Reynolds *et al* 2013, Smit *et al* 2013). The amount depends on ion chamber design and construction, its orientation in the field and the direction and magnitude of the magnetic field in relation to the radiation beam. Recent studies reported k_B factors, determined either by Monte Carlo calculations (O'Brien *et al* 2016, Spindeldreier *et al* 2017, Malkov and Rogers 2018, Pojtinger *et al* 2018) or by measurement of ion chamber readings with and without magnetic field (van Asselen *et al* 2018). Most of these studies assumed that k_Q in equation (4) can be taken from existing Codes of Practice, CoPs (Andreo *et al* 2000, Aalbers *et al* 2008, McEwen *et al* 2014). However, as shown by Woodings *et al* (2018), in case of the Elekta Unity MRI-linac used in this study, the flattening filter free (FFF) beam characteristics are affected by the MRI-cryostat wall. Consequently, the applicability of the k_Q from existing CoPs for application in MRI-linacs was never confirmed. In addition, despite the recommendation to measure k_Q against primary standards (Andreo *et al* 2000), which presumably also holds for k_B, no experimental data for k_Q or k_B based on primary standards in MRI-linacs is available. In order to do this ion chambers need to be calibrated in beam quality Q_0 (^{60}Co) without magnetic field to obtain N_{D_w,Q_0}, and in MRI-linac beam quality Q both with and without magnetic field to obtain respectively $N_{D_w,Q,B}$ and $N_{D_w,Q}$ in equation (4).

VSL developed a new water calorimeter as a primary standard for absorbed dose to water in ^{60}Co, kV and MV photon beams. It was designed to operate in a magnetic field of MRI incorporated treatment devices (de Prez *et al* 2016a). The calorimeter demonstrated its capability for on-site measurements in conventional flattened (cFF) and FFF high-energy photon beams (de Prez *et al* 2018b). Its international agreement for measurement of D_w in MV and ^{60}Co photon beams without magnetic field (i.e. at 0 T) and its uncertainty was confirmed by BIPM[4] key-comparisons (Picard *et al* 2017, Kessler *et al* 2018). A preliminary study showed its feasibility to measure absorbed dose to water, D_w, in a magnetic field and to calibrate ion chambers directly in the calorimeter phantom (de Prez *et al* 2016b). A more comprehensive study confirmed that the uncertainty for measurement of D_w with a water calorimeter in a 1.5 T magnetic field is estimated to be the same as under conventional reference conditions (de Prez *et al* 2019). The VSL water calorimeter is currently the only primary standard operable in a magnetic field that provides a direct link to the international system of units (SI).

The aim of this study is to measure k_Q and k_B directly for two ion chamber types of each three serial numbers in a pre-clinical 7 MV Elekta Unity MRI-linac at 0 T and at 1.5 T. This is done by direct D_w calibrations against the VSL primary standard in ^{60}Co, without magnetic field, and in beam quality Q, with and without magnetic field. Some of the materials and methods applied here, were described in detail earlier (de Prez *et al* 2016a, 2018a, 2019).

2. Materials and methods

2.1. The wide bore hybrid MRI-linac system

The pre-clinical Elekta Unity hybrid MRI-linac system comprised a modified 1.5 T Philips wide bore MRI with 70 cm diameter and an Elekta 7 MV standing wave linear accelerator producing an FFF photon beam with a pulse

[4] The Bureau Internationales des Poids et Mesures, BIPM in Sévres, is an international organization established by the Metre Convention, through which Member States act together on matters related to measurement science and measurement standards (www.bipm.org).

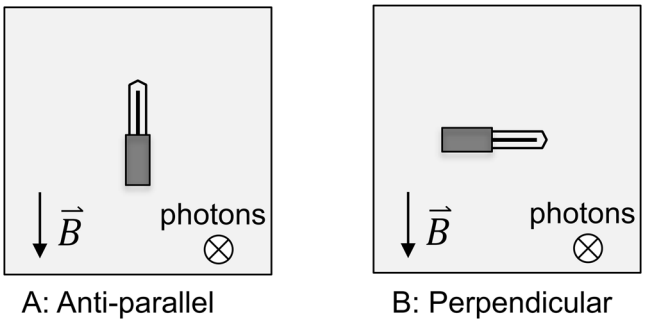

Figure 1. Vertical beam (gantry 0°) beam's-eye-views of the relative orientations of an ion chamber, magnetic field and beam direction for (A) antiparallel (|| 180°), and (B) perpendicular, (⊥ −90°, i.e. counter-clockwise), orientations.

rate frequency (PRF) of 275 Hz (Raaymakers *et al* 2009, Lagendijk *et al* 2014, Woodings *et al* 2018). A ring around the patient bore allowed for rotation with the accelerator iso-centre at 143.5 cm. It provided for a transverse magnetic field relative to the direction of the MV photon beam. The linac was equipped with an electronic portal imaging device (EPID), used for alignment of measurement equipment. The beam quality expressed in $TPR_{20,10}$ had a value of 0.701(2), independent of the presence of the magnetic field within its reported standard uncertainty (van Asselen *et al* 2018). All measurements in the current study were performed with a vertical beam, i.e. at gantry angle 0°.

2.2. The orientation dependence of $k_{Q,B}$

The effect on ion chamber responses due to the magnetic field, B, in beam quality Q, $k_{Q,B}$ in equation (4), is dependent on the orientation of the chamber and the direction of the magnetic field in relation to that of the beam. Hence, these conditions need to be specified to fully describe the relevant measurement conditions. It was shown previously that chamber orientations with the thimble facing in opposite direction (or the magnetic field sign changed) can result in a different chamber response. This is caused by a non-symmetric, chamber dependent dead-volume near the chamber guard electrode, i.e. at the stem-side (Butler *et al* 2015, Malkov and Rogers 2017, Spindeldreier *et al* 2017). It is caused by the design of modern ion chambers. The orientations applied in this study are illustrated in figure 1.

2.3. Calorimetric determination of D_w

The D_w measurements are described elsewhere (de Prez *et al* 2019). Measurements at 1.5 T took place on day, 1, 2, 3 and 19 of a 19 d period (six measurement series). The MRI-linac magnet was ramped down on day 22 and calorimeter measurements were repeated at 0 T on day 23, 24, and 34 (three measurement series). The measurements were performed in groups of approximately $N = 30$ consecutive calorimeter runs, taking about 5 min per run of which 1 min of irradiation. On three occasions, two with magnetic field and one without magnetic field, the orientation of the calorimeter high-purity water cell was changed from perpendicular to parallel as described previously (de Prez *et al* 2019). Each time this was done on the same day. It was shown earlier that the calorimeter performance, both with and without magnetic field, was unaffected by the orientation of the vessel. Therefore, in this study, perpendicular and parallel measurements with magnetic field were combined for their contribution to D_w. The same was done for perpendicular and parallel measurement without magnetic field.

2.4. Ion chamber calibration

Ion chamber calibrations at 1.5 T were done in the period between day 4 and day 18 and at 0 T in the period between day 25 and day 33, both preceded and succeeded by calorimeter D_w measurements. Prior to the ion chamber calibration, all chambers were imaged by CT and no irregularities in chamber construction were observed. The ion chamber signal, M, was integrated over 60 s, the same integration time as used for the calorimetric D_w measurements, descripted earlier (de Prez *et al* 2019). This was done to avoid introduction of differences in beam on-off timing between calorimetry and ion chamber measurements. Furthermore, the ion chambers signal was measured in the same set-up as the D_w measurements, i.e. inside the calorimeter water phantom, however, with the water at room temperature. The corrected ion chamber reading, M, in equation (1) was determined by:

$$M = \left(M_{raw} - M_{leakage}\right) \cdot k_{elec} \cdot k_{p,T} \cdot k_s \cdot k_{pol} \cdot k_R, \tag{5}$$

where the leakage signal, $M_{leakage}$, in the electrometer readings, M_{raw}, was shown to be negligible (<0.05%). The reading was corrected for electrometer calibration, k_{elec}, air cavity density compared to reference air density, $k_{p,T}$, incomplete charge collection due to recombination, k_s and chamber polarity, k_{pol}. Temperature was measured in

water, close to the ion chamber thimble. The air pressure was measured in the linac room at the approximate ion chamber height. Deviation from geometrical reference conditions and to the dose at the central axis of the beam was corrected for by k_R:

$$k_R = k_{SDD} \cdot k_d \cdot k_v, \quad (6)$$

which contains corrections to reference source detector distance (SDD), k_{SDD}, specific depth (in g cm^{-2}) in water, k_d, and correction for volume averaging over the length of the ion chamber cavity, k_v.

The ion chamber collecting potential, supplied to the central electrode by the electrometer (Keithley 6517B), was set to −300 V. In the MRI-linac, the ion recombination correction, k_s, was measured by applying the method described by Weinhous and Meli (1984) as recommended by commonly used Codes of Practice (Andreo *et al* 2000) with a collecting potential of −100 V directly following a measurement with a collection potential of −300 V. This method was shown to be independent of magnetic field (Smit *et al* 2013). In the beam quality Q_0, ^{60}Co, the ion recombination was measured by applying the method described by Boutillon (1998) for continuous beams. For all beams, the polarity correction, k_{pol}, was applied according to the methods described by e.g. Andreo *et al* (2000), performing measurements at +300 V collecting potential.

No additional correction was applied for the air attenuation between the monitor ion chamber and the calorimeter, since the variation of the correction with varying ambient conditions was small. No correction was applied for air relative humidity since all measurements took place at a relative humidity between 25% and 60% for which no correction is needed (Bichsel *et al* 1979, McEwen and Taank 2017). SDD of the instruments, i.e. ion chambers and calorimeter, was within 0.2 cm from the nominal SDD of 139.3 cm, 4.2 cm above iso-centre. The depth of the instruments was within 0.06 g cm^{-2} from the nominal value of 10 g cm^{-2}. SDD and depth were corrected to the nominal values by inverse square law and effective attenuation, μ (0.036 cm^2 g^{-1} based on a $TPR_{20,10}$ of 0.70), as described by Andreo *et al* (2017), respectively k_{SDD} and k_d in equation (6). The field size of the beam was set to 10 × 10 cm^2 at the iso-centre, corresponding to 9.7 × 9.7 cm^2 at the measurement position. The correction to the central axis-profile was applied by the ion chamber volume averaging correction, k_v by a simple integration of the lateral beam profile over the length of the ion chamber cavity and normalization to central axis dose as described by Palmans *et al* (2017). In this study k_v was applied separately and not included in k_Q because the available k_Q literature value to compare to was also determined without inclusion of k_v (Malkov and Rogers 2018).

The ion chambers were calibrated in both antiparallel (|| 180°) and perpendicular (⊥ −90°) direction in a 1.5 T magnetic field, illustrated in figure 1. After ramp down, the calibrations were repeated at 0 T.

2.5. Ion chamber positioning

The ion chambers were positioned inside the calorimeter phantom by methods described elsewhere (de Prez *et al* 2016a). To prevent variations in reading due to air around the ion chamber waterproofing sleeves (Hackett *et al* 2016), all measurements were performed directly in water using waterproof ion chambers. The black line on the stem of the ion chambers was facing the radiation source. After measurement in perpendicular orientation (figure 1(B), ⊥ −90°), the ion chambers orientations were remotely rotated 90° around the beam-axis to antiparallel orientation (figure 1(A), || 180°) without the need to access the water phantom. The difference between SDD in both orientations was negligible (<0.05 mm). The difference in ion chamber SDD, compared to calorimeter SDD, was measured with an uncertainty of 0.3 mm ($k = 1$), equivalent to a relative standard uncertainty of 0.05% on the determination of k_{SDD} in equation (6). This was slightly larger than in conventional linacs where it was considered to be 0.02% (de Prez *et al* 2016a). The uncertainties in the depth and volume averaging correction, k_d and k_v was the same as reported earlier (de Prez *et al* 2016a, 2018b), respectively 0.04% and 0.05% ($k = 1$).

2.6. Beam output monitoring

The D_w and ion chamber measurements performed in this study took place over a period of several weeks. Therefore, an independent beam output monitor was used to normalize the measurement of D_w and M for determination of $N_{D_w,Q,B}$ and, after ramp-down $N_{D_w,Q}$ in equation (4). The monitor system was described in detail earlier (de Prez *et al* 2019), where an additional standard uncertainty of 0.16% was applied for the monitor day-to-day variations.

2.7. Consistency check by independent posterior cross-calibration

The ion chamber measurements in the calorimeter water phantom are potentially sensitive to errors that can be made due to e.g. unnoticed geometrical misalignment, displacement of the transmission monitor, air-bubbles around the chamber or other unwanted effects. To validate ion chamber measurement in the calorimeter, an independent consistency check was done by cross-calibrating the ion chambers in an independent experiment. This was done after the calorimeter set-up was removed from the bore and the patient couch was re-installed. Each ion chamber was cross-calibrated against the other five. The cross-calibration was performed in such a way

that most of the correction factors from equations (5) and (6) canceled. The cross-calibrations were performed at 0 T and, after magnet ramp-up, at 1.5 T in the orientations shown in figure 1, i.e. antiparallel (|| 180°) and perpendicular (⊥ −90°). Measurements were performed in a modified MRI-compatible PTW MP1 water phantom, placed on the patient couch. The chambers were positioned at the iso-centre (143.5 cm), at a nominal depth of 10 cm. The black line on the stem of the ion chamber was facing the radiation source. At the same depth, approximately 2 cm off-centre, a waterproof IBA CC13 ion chamber was used as an independent monitor chamber. The ion chambers were connected to PTW Unidos E electrometers. All ion chamber readings were recorded in the same set-up. For each ion chamber, j, the calibration coefficient, $N_{D_w}^{\text{cross},j}$, was determined according to:

$$N_{D_w}^{\text{cross},j} = \frac{1}{5} \cdot \frac{\sum_{i \neq j} \left(N_{D_w}^{\text{wcm},i} \cdot M_i \cdot k_{s,i} \cdot k_{\text{pol},i} \right)}{M_j \cdot k_{s,j} \cdot k_{\text{pol},j}}. \quad (7)$$

The average of absorbed dose, D_w, based on measurement with the other five chambers ($i \neq j$) was based on their calibration coefficients measured in the water calorimeter, $N_{D_w}^{\text{wcm},i}$, and represented by one fifth of the value of the numerator of the right-hand side of equation (7). Leakage signal, M_{leakage}, in the electrometer readings, M_{raw}, according to equation (5) was shown to be negligible (<0.05%). Corrections for polarity, k_{pol}, and recombination, k_s, were applied according to the methods described earlier. The corrections for $k_{p,T}$ in equation (5) and k_{SDD} and k_d in equation (6) were not considered relevant because the monitor ion chamber was in a fixed geometry and therefore affected in the same way by variations in temperature, pressure, SDD and depth. Additionally, ion chamber volume averaging effect, k_v in equation (6) was shown to be the same for all chambers and therefore not applied. Despite the different SDD and thus a slightly different beam size at the position of the ion chamber than used during the measurements in the calorimeter phantom, differences in ion chamber stem corrections between the two chamber types were considered negligible. Corrections for electrometer calibration, k_{elec}, were not applied since all ion chambers were measured with the same electrometer, at the same range and with the same collection potential (−250 V) applied. All ion chambers measurements at either 0 T and 1.5 T were performed on the same day.

Due to the nature of this experimental set-up measured ratios of ion chamber readings at either 0 T or 1.5 T were potentially more reliable than those in the calorimeter phantom. Therefore, erroneous results of a single chamber measurement in the calorimeter dataset could be detected as an outlier using this method. Note that direct transfer of the calorimetric D_w was not possible because different monitor ion chambers were used in both the calorimeter and the cross-calibration set-up. Note that equation (7) could have been expressed as ratios of chamber readings. However, it was chosen to express the values in terms of calibration coefficients because k_B values are based on a ratio of calibration coefficients according to equation (4).

3. Results

3.1. Calorimeter D_w measurements

Calorimetric determination of D_w are shown in table 1 and figure 2. For each group of ~30 runs the mean and the standard deviation (SD) was determined. The standard deviation of the mean, SDOM, was calculated for the groups based on the square root of N. It was shown to be less than 0.1% and independent of the magnetic field. Additionally, the mean of the respective six and three groups was determined and the related SD of the group of these means was calculated, referred to as the 'actual SD of the means' or 'actual SDOM'. The 'actual SDOM' was respectively 0.26% and 0.08% for the six groups of D_w measurements with magnetic field and three groups of D_w measurements without magnetic field. If no additional day-to-day variation would be present, the SDOM should be the same as the 'actual SDOM'. This is the case for the measurements without magnetic field. However, with magnetic field, the 'actual SDOM' is larger than the SDOM, indicating an additional day-to-day variation in the D_w measurements. This effect was also found in a previous study (de Prez *et al* 2019), where the day-to-day variation was presumably caused by the transmission monitor set-up in the MRI-linac with magnetic field and amounted to 0.16% for measurements over a period of 4 days (de Prez *et al* 2019). In the current study, the calorimeter measurements with magnetic field took place at the start and end of a 19 day period. The D_w measurements, performed over the first days at the beginning of the respective periods were shown to be closer together than the final D_w measurements. This indicates the presence of a long-term (>10 d) day-to-day variation, larger than 0.16%, previously determined over a period of 4 days. To account for this in the current study, the measured 'actual SDOM' is applied as the Type A uncertainty contribution, i.e. determined by repeated measurement, to the D_w for determination of the ion chamber magnetic field correction factor, k_B. No additional day-to-day variation on the ion chamber measurements was applied, because this was accounted for by the variation in calorimetric D_w measurements. The dose-rate at the calorimeter reference conditions before

Table 1. Summary of D_w measurements at 1.5 T and at 0 T, normalized to the applied transmission monitor, D_w/MU in cGy μC^{-1}, during the 30 days measurement period in the MRI-linac.

Normalized D_w at 1.5 T						Normalized D_w at 0 T					
Day	‖/⊥	N	D_w/MU/ cGy μC^{-1}	SD/%	SDOM/%	Day	‖/⊥	N	D_w/MU/ cGy μC^{-1}	SD/%	SDOM/%
#1	‖	28	65.31	0.49	0.09	#23	‖	30	61.48	0.40	0.07
#2	‖	29	65.36	0.42	0.08	#24	⊥	29	61.49	0.32	0.06
#2	⊥	22	65.50	0.32	0.07	#34	‖	30	61.40	0.33	0.06
#3	⊥	38	65.41	0.41	0.07						
#3	‖	20	65.33	0.53	0.12						
#19	‖	30	65.00	0.47	0.09						
Group			65.32	0.26[a]		Group			61.46	0.08[b]	

[a] Average and SD of six measurement series, performed on days #1, #2, #3 and #19 at 1.5 T.
[b] Average and SD of three measurement series at 0 T, performed on days #23, #24 and #34.

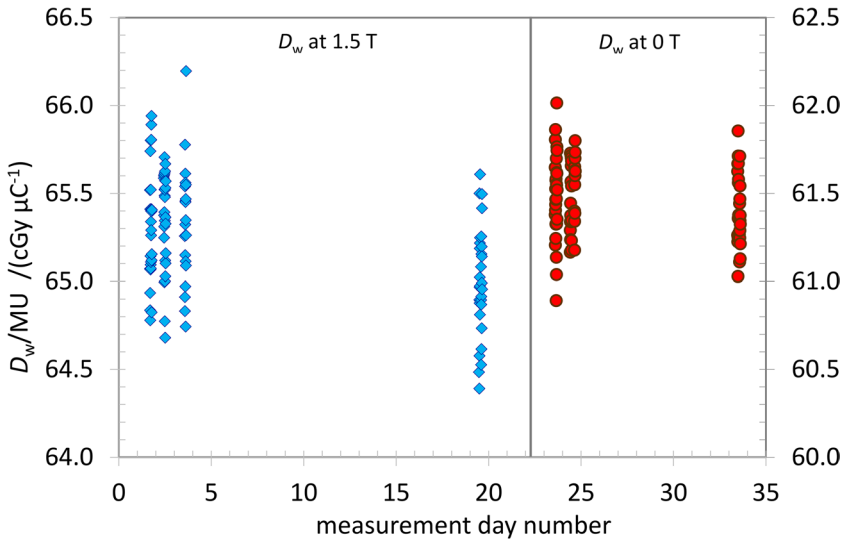

Figure 2. D_w measurements, normalized to the applied transmission monitor, D_w/MU in cGy μC^{-1}, before and after MRI-linac ramp-down.

Table 2. Ion chamber correction factors for recombination, k_s, and polarity, k_{pol}, in the MRI-linac. Differences in k_s and k_{pol} in different orientations were smaller than 0.05%.

Chamber	beam	B-field	k_s	k_{pol}
PTW 30013	X7	1.5 T	1.0053(5)	1.0000(4)
		0 T	1.0047(1)	1.0002(3)
	^{60}Co	0 T	1.0010(2)	1.0002(3)
IBA FC65-G	X7	1.5 T	1.0060(4)	0.9989(4)
		0 T	1.0054(1)	0.9991(2)
	^{60}Co	0 T	1.0007(2)	0.9991(1)

and after ramp-down was approximately 9.4 cGy s^{-1}, which relates at a 275 Hz PRF to a water absorbed-dose-per-pulse of approximately 0.34 mGy pulse^{-1}.

3.2. Ion chamber measurements

The ion chamber correction factors from equation (5), except for k_{elec}, $k_{p,T}$ and k_R, are given in table 2. For all Farmer type chambers applied in this study with the same nominal cavity length of 2.3 cm, the volume averaging correction, k_v, from equation (6) was 1.0022(5) with magnetic field and 1.0023(5) without magnetic field. These values were in agreement with a volume averaging correction of 1.0021 calculated with a generic equation for FFF beams given by Palmans *et al* (2017). Despite a slight difference in beam profile between the lateral x and

Table 3. Uncertainty budget for k_Q and k_B factors in this study. All uncertainties are of Type B, except for the repeated chamber measurements, M/MU.

	k_Q		k_B	
Source of uncertainty Measurement:	^{60}Co: 0 T	Q: 0 T	Q: 0 T	Q: 1.5 T
D_w/MU, contribution to k_B and k_Q measurements	0.20	0.08	0.08	0.26
Charge measurement per monitor unit (M/MU), Type A	0.10		0.10	
Corrections for saturation and polarity, k_s and k_{pol}	0.07		0.07	
Correction for p, T, $k_{p,T}$ and relative humidity	0.15		0.15	
Correction to reference SDD, k_{SDD}	0.02	0.05	0.05	
Correction to reference depth in water, k_d	0.04		0.04	
Relative combined standard uncertainty ($k = 1$)	0.30		0.34	

y directions, k_v, was not significantly different between the two chamber orientations. In the current study, the corrections k_{SDD} and k_d were always smaller than 0.27% and usually smaller than 0.10%. Uncertainties for the contributions to k_R in equation (6) are presented elsewhere (de Prez *et al* 2016a, 2018b). Measurement of k_s and k_{pol} in the MRI-linac were done immediately following the ion chamber calibrations. The average values per chamber type are given in table 2. With and without magnetic field, all measurements were done in perpendicular ($\perp -90°$) and antiparallel ($||\ 180°$) direction to the bore.

3.3. Uncertainties in ion chamber k_Q and k_B factors

The uncertainty budget for D_w measurements with and without magnetic field was presented earlier (de Prez *et al* 2016a). It was shown that measurement of D_w with a water calorimeter and its related uncertainties are independent of the magnetic field, except for the larger Type A uncertainty in the repeated D_w/MU measurements, caused by the monitor set-up in the magnetic field. Therefore, the Type A uncertainty of 0.20% for repeated $\Delta R/R$ measurements in table 3 of de Prez *et al* (2016a), was replaced by the Type A uncertainties of the current study, respectively 0.26% and 0.08%. Furthermore, the uncertainty in correction to reference SDD k_{SDD} was adjusted from 0.02% to 0.05% caused by the alignment of the calorimeter in the MRI-linac bore. For the current study, this led to relative standard uncertainties in D_w for measurements at 1.5 T and at 0 T of respectively 0.53% and 0.38% ($k = 1$). The uncertainty in k_B and k_Q in this study was established in the same way as described earlier, taking correlation between the dose measurements in the denominator and nominator of equation (3) into account (de Prez *et al* 2016a, 2018b). The calorimetric contributions to the uncertainties in k_B and k_Q are shown in the first row of table 3. The 'actual SDOM' of calorimeter measurements, shown in table 1, is applied as the Type A uncertainty on determination of D_w. The uncertainty for the ion chamber beam quality corrections at 0 T, k_Q, is determined as the quadratic sum of the contributions reported in table 3 under ^{60}Co and Q. The uncertainty for the ion chamber magnetic field corrections at 1.5 T, k_B is determined as the quadratic sum reported in the table under Q and B at 1.5 T. The differences in uncertainty contributions to the SDD in ^{60}Co and in the MRI-linac were accounted for in k_Q because of the measurement in different facilities and therefor correlations do not apply. This means that 0.02% and 0.05% is accounted for in k_Q while only 0.05% is accounted for in k_B. No distinction is made between the uncertainties in k_B factors for chambers placed in either antiparallel or perpendicular orientation to magnetic field. The uncertainty in $k_{Q,B}$ is determined in a similar way to be 0.39%, but not shown in table 3. No uncertainty contribution was applied for the response change as a result of chamber misalignment with respect to its angle, which was expected to be smaller than 0.05% based on a potential misalignment smaller than 0.5° (Smit *et al* 2013).

3.4. Ion chamber consistency checks

Table 4 shows the ion chamber calibration coefficients, N_{D_w}, of the six ion chambers based on direct calibration with the water calorimeter. Corresponding measurements without magnetic field were combined because no significant differences were seen between the chamber orientations. The table also shows the results of the additional cross-calibration, performed after removal of the calorimeter equipment from the MRI-linac bore. These results are expressed as relative deviations compared to the direct calibration coefficients, $\Delta_{N_{D_w,Q}}$, where each chamber was cross-calibrated against the other five ion chambers. Per chamber type, field strength and chamber orientation, the standard deviation (SD) of the respective $\Delta_{N_{D_w,Q}}$ for the three corresponding calibration coefficients is reported. Table 4 shows that for individual chambers, deviations are mostly smaller than 0.10% and for some chambers about 0.25%. However, for chamber PTW 30013 with serial number 008474, deviations with magnetic field antiparallel and perpendicular are respectively +0.50% and −0.44% which influences respectively the $k_{B||}$ and $k_{B\perp}$ by the same amount. For the measurements without magnetic field,

Table 4. Direct calibration coefficients for the six ion chambers measured without magnetic field, $N_{D_w,Q}$, and with magnetic field in antiparallel and perpendicular orientation, respectively $N_{D_w,Q,B||}$ and $N_{D_w,Q,B\perp}$. The results of the cross-calibration are expressed as the relative deviations compared to the direct calibrations in the water calorimeter, $\Delta_{N_{D_w,Q}}$. The cross-calibration coefficients were based on the same calorimeter D_w values as the direct calibration coefficients.

Chamber	sn	$N_{D_w,Q}$/ (mGy pC^{-1})	$\Delta_{N_{D_w,Q}}$/%	$N_{D_w,Q,B\|\|}$/ (mGy pC^{-1})	$\Delta_{N_{D_w,Q,B\|\|}}$/%	$N_{D_w,Q,B\perp}$/ (mGy pC^{-1})	$\Delta_{N_{D_w,Q,B\perp}}$/%
PTW 30013	007120	52.53	+0.07	52.04	−0.15	50.65	+0.24
	008377	52.74	−0.03	51.81	−0.01	50.66	+0.04
	008474	52.52	+0.02	51.54	+0.50	50.68	−0.44
	SD		0.05		0.34		0.35
IBA FC65-G	3129	47.50	−0.08	47.20	+0.02	45.29	+0.16
	3212	47.52	+0.03	47.38	−0.25	45.52	−0.04
	3213	47.40	+0.05	47.19	−0.11	45.29	+0.06
	SD		0.07		0.14		0.10

Table 5. This study's ion chamber k_Q and k_B factors with magnetic field in antiparallel (|| 180°) orientation and perpendicular (⊥ −90°), orientation. $k_{Q,B}$ factors can be obtained by multiplication of k_Q and k_B.

			k_B	
Chamber	sn	k_Q	||	⊥
PTW 30013	007120	0.985	0.991	0.964
	008377	0.988	0.982	0.961
	008474	0.982	0.982	0.965
	SD /%	0.3	0.5	0.2
	generic	0.985(5)	0.985(6)	0.963(4)
IBA FC65-G	3129	0.990	0.994	0.953
	3212	0.993	0.997	0.958
	3213	0.987	0.996	0.956
	SD /%	0.3	0.2	0.2
	generic	0.990(5)	0.995(4)	0.956(4)

SDs of the differences are smaller than 0.10%. SDs for measurements with magnetic field are larger and range between 0.10% and 0.35%. Similar to the D_w/MU measurements, SDs without magnetic field are smaller than with magnetic field. Pojtinger *et al* (2018) also observed larger day-to-day variation for their experiments with Farmer type ion chambers in a magnetic field for which the reason remained unresolved. However, based on the SDs given in table 4, it can be concluded that the individual ion chamber measurements show an adequate consistency as a basis for the generic k_Q and k_B data per chamber type, reported in table 5. Therefore, no direct calorimeter calibrations were rejected.

3.5. Ion chamber k_Q and k_B factors

Ion chamber k_Q and k_B values and their uncertainties are given in table 5. Ion chamber calibrations were based on the calorimetric D_w measurements with the high-purity cell in antiparallel as well as perpendicular direction to the bore, both with and without magnetic field. The ^{60}Co measurements at 0 T, before and after the measurements at the MRI-linac, were performed in a similar way as described earlier (de Prez *et al* 2016a). k_B values were entirely based on the measurements done at 1.5 T, before magnet ramp-down and at 0 T, just after magnet ramp-down. Therefore, the reported k_B is independent on the ^{60}Co measurements. Variation of D_w in ^{60}Co, used for determination of k_Q, before and afterwards was smaller than 0.05%, confirming a chemically stable HPC and thermistor calibration during the measurements in the MRI-linac. The uncertainties on the generic k_Q and k_B values are established by adding the uncertainties reported in table 3 to the relative standard deviation, SD, reported in table 5. $k_{Q,B}$ factor can be obtained by multiplication of k_Q and k_B according to equation (4).

Based on the cross-calibration dataset, presented in table 4, ratios between chamber calibration coefficients and thus between chamber k_Q and k_B values were verified in the same way. Consistency of generic k_Q and k_B values were shown to be always smaller than 0.11% with SDs smaller than 0.14%.

Table 6. This study's ion chamber k_Q and k_B factors compared to available literature values. Note that the Monte Carlo studies included the ion chamber sensitive volume, indicated with SV (Butler *et al* 2015, Malkov and Rogers 2017, Spindeldreier *et al* 2017) in the calculation of k_B, which is intrinsically incorporated in the measured k_B values.

Chamber	Study	Method	k_Q	$k_{B\parallel}$	$k_{B\perp}$
PTW 30013	van Asselen *et al* (2018)	Measured	—	0.992(2)	0.963(2)
	Malkov and Rogers (2018)	Monte Carlo—SV	0.984(1)	0.988(1)	—
	Pojtinger *et al* (2018)	Monte Carlo	—	0.996(2)	—[a]
	Spindeldreier *et al* (2017)	Monte Carlo—SV	—	0.993(3)	0.954(3)
	O'Brien *et al* (2016)	Monte Carlo	—	0.994(1)	0.976(1)
	Mean (SD)		—	0.993(3)	0.964(11)
	Difference from this study		−0.1(5)%	+0.8(7)%	+0.1(12)%
IBA FC65-G	van Asselen *et al* (2018)	Measured	—	0.997(3)	0.952(2)
	Malkov and Rogers (2018)	Monte Carlo—SV	0.988(1)	0.992(1)	—[a]
	Mean (SD)		—	0.995(4)	0.952(2)
	Difference from this study		−0.2(5)%	−0.1(6)%	−0.4(5)%

[a] These studies reported values in perpendicular direction to the magnetic field, however with the chamber in opposite orientation to the other studies reported in the table. It was shown in the reported studies that 'perpendicular' and 'anti-perpendicular' value for k_B could give different results. Therefore, these values are not reported here.

4. Discussion

4.1. Measurement of k_Q and k_B

k_Q and k_B values for ion chambers, reported in table 5, were measured with uncertainties of respectively 0.30% and 0.34%, given in table 3. The major contribution to these uncertainties were of Type A, obtained from repeated calorimeter measurements, D_w/MU, in ^{60}Co and in the MRI-linac with magnetic field. The Type A uncertainty in the calorimeter measurements with magnetic fields (0.26%) was higher than that without magnetic field (0.08%). This was presumably caused by day-to-day variations in normalization due to the transmission monitor set-up inside the magnetic field of the MRI-linac (de Prez *et al* 2019). To reduce this uncertainty contribution for future measurement the independent monitor set-up needs to be improved. Other uncertainty contributions in the MRI-linac determination of k_Q, are the same as in conventional linac beams, except for the uncertainty in correction to reference SDD, k_{SDD}. This was adjusted from 0.02% to 0.05% due to the alignment of the calorimeter in the MRI-linac bore. Ion chamber corrections for volume averaging, k_v were smaller than previously measured in conventional FFF beams and larger than those in beams with flattening filter (de Prez *et al* 2018b). This was mainly caused by beam flattening due to an increased SDD in the MRI-linac (139.3 cm) compared to the SDD in conventional linacs as given by Palmans *et al* (2017). Corrections for recombination and polarity, presented in table 2, confirm that, for the applied ion chambers, the polarity correction is both independent on beam modality and magnetic field within the reported uncertainty. k_s in a continuous beam of ^{60}Co is very small (<0.1%) as expected and mainly caused by initial recombination (Boutillon 1998). A consistency check by independent cross-calibration of each ion chamber against the other five, showed adequate consistency as a basis for the generic k_Q and k_B data per chamber type as reported in table 5. However, also here the measurements with magnetic field showed a larger SD than without magnetic field.

4.2. Comparison of k_Q and k_B with current literature

k_Q factors were determined independent of chamber orientation. k_B factors were determined in two orientations, antiparallel ($\parallel -90°$) and perpendicular ($\perp 180°$) to the transverse magnetic field. Table 6 gives currently reported literature values. All currently available values were reported with their Type A uncertainties only. The values summarized in table 6 represent the unweighted means, which assumes that the overall uncertainties of the reported values (i.e. Type A plus Type B uncertainties) are very close to each other. Differences between beam profiles with and without magnetic field are not considered to affect k_B factors. The study by Malkov and Rogers (2018) is the only study that also reports Monte Carlo calculated k_Q values for the same ion chambers and MRI-linac as applied in the current study at 0 T. The other studies assume that k_Q values for the MRI-linac can be taken from existing CoPs, which is not trivial because the MRI-linac FFF beam is affected by the MRI-cryostat (Woodings *et al* 2018). Differences in ion chamber volume averaging, k_v, must be considered when comparing k_Q values. In the current study, k_Q values in table 6 did not include chamber volume averaging effect. Table 6 gives the differences between the mean of the earlier reported values in literature and the values obtained in the current study. Differences for k_B range from −0.4% to +0.8%. Differences in k_Q based only on one study (Malkov and Rogers 2018) are smaller than 0.2%. All results are well within the expanded uncertainties ($k = 2$)

of their differences. The largest difference from literature of 0.8% is observed for the $k_{B\perp}$ of the PTW 30013 type. However, this value is consistent with the performed cross-calibration against the other five ion chambers and there is no reason to reject this value. In general, it can be concluded that the values presented in table 5 are currently the best estimates provided with a comprehensive uncertainty budget for k_Q and k_B, both || 180° and ⊥ −90°, in the Elekta Unity 7 MV MRI-linac.

The only studies basing their results on measurements are the current study and the study by van Asselen *et al* (2018). It is known that the chamber sensitive volume described by Butler *et al* (2015) plays a significant role in k_B and subsequently the orientation of the chamber in the magnetic field (Malkov and Rogers 2017, Spindeldreier *et al* 2017). This must be accounted for correctly when calculating k_B by Monte Carlo methods. The reported Monte Carlo studies only accounted for this in a quantitative way, i.e. based on matching Monte Carlo calculations with experiments. However, since the exact ion chamber dead-volume is currently unknown and is dependent of chamber guard construction, thus chamber type, this introduces an increased Type B uncertainty in the calculations. This is not covered by the reported uncertainties of the current Monte Carlo studies.

5. Conclusion

This study reports, for the first time, measured k_Q factors at 0 T and k_B factors at 1.5 T in a 7 MV photon beam of a pre-clinical Elekta Unity MRI-linac. The measurements were based on direct calibrations, traceable to the Dutch primary standard for absorbed dose to water, operated on-site in the bore of the MRgXT device. Despite variations in measurements with magnetic field, the values presented are currently the best estimated provided with a comprehensive uncertainty budget for generic k_Q and k_B, both antiparallel (|| 180°) and perpendicular (⊥ −90°), for PTW 30013 and IBA FC65-G chambers in the Elekta Unity MRI-linac. Partly because of the relatively large SD of the available literature values (up to 1%), agreement was shown with the values presented in the current study.

Acknowledgments

This project has received funding from the EMPIR programme, grant 15HLT08 'Metrology for MR guided Radiotherapy', co-financed by the Participating States and from the European Union's Horizon 2020 research and innovation programme.

ORCID iDs

Leon de Prez https://orcid.org/0000-0002-7470-4356
Jacco de Pooter https://orcid.org/0000-0002-7542-257X

References

Aalbers A H L, Hoornaert M-T, Minken A, Palmans H, Pieksma M W H, De Prez L A, Reynaert N, Vynckier S and Wittkämper F W 2008 Code of practice for the absorbed dose determination in high energy photon and electron beams *Technical Report* NCS 18 (The Netherlands: Nederlandse Commissie voor Stralingsdosimetrie, NCS) (https://doi.org/10.25030/ncs-018)

Almond P R, Biggs P J, Coursey B M, Hanson W F, Huq M S, Nath R and Rogers D W O 1999 AAPM's TG-51 protocol for clinical reference dosimetry of high-energy photon and electron beams *Med. Phys.* **26** 1847–70

Andreo P 1992 Absorbed dose beam quality factors for the dosimerty of high-energy photon beams *Phys. Med. Biol.* **37** 2189–211

Andreo P *et al* 2000 Absorbed Dose Determination in External Beam Radiotherapy *Technical Report* IAEA TRS-398 (Vienna: International Atomic Energy Agency)

Andreo P, Burns D, Nahum A, Seuntjens J and Attix F H 2017 *Fundamentals of Ionizing Radiation Dosimetry* (New York: Wiley)

Bichsel H, Pierson D H, Boring J W, Green A, Inokuti M, Hurst G and ICRU 1979 Average Energy Required to Produce an Ion Pair 31 *Technical Report* ICRU 31 (Washington, DC: International Commission on Radiation Units & Measurements)

Boutillon M 1998 Volume recombination parameter in ionization chambers *Phys. Med. Biol.* **43** 2061–72

Butler D J, Stevenson A W, Wright T E, Harty P D, Lehmann J, Livingstone J and Crosbie J C 2015 High spatial resolution dosimetric response maps for radiotherapy ionization chambers measured using kilovoltage synchrotron radiation *Phys. Med. Biol.* **60** 8625–41

de Prez L A, de Pooter J A, Jansen B J, Aalbers T and Aalbers A H L 2016a A water calorimeter for on-site absorbed dose to water calibrations in ^{60}Co and MV-photon beams including MRI incorporated treatment equipment *Phys. Med. Biol.* **61** 5051–76

de Prez L A, de Pooter J A, Jansen B J, Woodings S J, Wolthaus J W H, van Asselen B, van Soest T L, Kok J G M and Raaymakers B W 2019 Commissioning of a water calorimeter as a primary standard for absorbed dose to water in magnetic fields *Phys. Med. Biol.* **64** 035013

de Prez L, de Pooter J, Jansen B, Perik T and Wittkämper F 2018b Comparison of K_Q factors measured with a water calorimeter in flattening filter free (FFF) and conventional flattening filter (cFF) photon beams *Phys. Med. Biol.* **63** 045023

de Prez L, de Pooter J, Jansen B, Wolthaus J, van Asselen B, Woodings S, Soest T, Kok J and Raaymakers B 2016b TH-CD-BRA-05: first water calorimetric D_w measurement and direct measurement of magnetic field correction factors, $K_{Q,B}$, in a 1.5 T B-field of an MRI linac *Med. Phys.* **43** 3874

de Prez L, Heukelom S, Jansen B, Jansen W, van de Kamer J, van Klink W, Kok E, Perik T, de Pooter J and Wittkämper F 2018a An on-site dosimetry audit for high-energy electron beams *Phys. Imaging Radiat. Oncol.* **5** 44–51

Fallone B G 2014 The rotating biplanar linac-magnetic resonance imaging system *Semin. Radiat. Oncol.* **24** 200–2

Hackett S L, van Asselen B, Wolthaus J W H H, Kok J G M M G, Woodings S J, Lagendijk J J W W and Raaymakers B W 2016 Consequences of air around an ionization chamber: are existing solid phantoms suitable for reference dosimetry on an MR-linac? *Med. Phys.* **43** 3961–8
Keall P J, Barton M and Crozier S 2014 The Australian magnetic resonance imaging-linac program *Semin. Radiat. Oncol.* **24** 203–6
Kessler C, Burns D, Jansen B J, Pooter J A de and Prez L A de 2018 Comparison of the standards for absorbed dose to water of the VSL, The Netherlands, and the BIPM for ^{60}Co γ rays *Metrologia* **55** 06012
Lagendijk J J W, Raaymakers B W and van Vulpen M 2014 The magnetic resonance imaging-linac system *Semin. Radiat. Oncol.* **24** 207–9
Malkov V N and Rogers D W O 2017 Sensitive volume effects on Monte Carlo calculated ion chamber response in magnetic fields *Med. Phys.* **44** 4854–8
Malkov V N and Rogers D W O 2018 Monte Carlo study of ionization chamber magnetic field correction factors as a function of angle and beam quality *Med. Phys.* **45** 908–25
McEwen M R and Taank J 2017 Examining the influence of humidity on reference ionization chamber performance *Med. Phys.* **44** 694–702
McEwen M, DeWerd L, Ibbott G, Followill D, Rogers D W O, Seltzer S and Seuntjens J 2014 Addendum to the AAPM's TG-51 protocol for clinical reference dosimetry of high-energy photon beams *Med. Phys.* **41** 041501
Meijsing I, Raaymakers B W, Raaijmakers A J E, Kok J G M, Hogeweg L, Liu B and Lagendijk J J W 2009 Dosimetry for the MRI accelerator: the impact of a magnetic field on the response of a Farmer NE2571 ionization chamber *Phys. Med. Biol.* **54** 2993–3002
Mutic S and Dempsey J F 2014 The viewray system: magnetic resonance-guided and controlled radiotherapy *Semin. Radiat. Oncol.* **24** 196–9
O'Brien D J, Roberts D A, Ibbott G S and Sawakuchi G O 2016 Reference dosimetry in magnetic fields: formalism and ionization chamber correction factors *Med. Phys.* **43** 4915–27
Oborn B M, Metcalfe P E, Butson M J and Rosenfeld A B 2010 Monte Carlo characterization of skin doses in 6 MV transverse field MRI-linac systems: effect of field size, surface orientation, magnetic field strength, and exit bolus *Med. Phys.* **37** 5208–17
OIML 2007 *International Vocabulary of Metrology—Basic and General Concepts and Associated Terms (VIM)* 3rd edn (Paris: Bureau International des Poids et Mesures)
Palmans H, Andreo P, Saiful Huq M, Seuntjens J, Vatnitsky S, Meghzifene A and Christaki K 2017 Dosimetry of Small Static Fields Used in External Beam Radiotherapy *Technical Report* IAEA-AAPM TRS-483 (Vienna: International Atomic Energy Agency)
Picard S, Burns D T, Roger P, Prez L A de, Jansen B J and Pooter J A 2017 Key comparison BIPM.RI(I)-K6 of the standards for absorbed dose to water of the VSL, Netherlands and the BIPM in accelerator photon beams *Metrologia* **54** 06005
Pojtinger S, Dohm O S, Kapsch R-P and Thorwarth D 2018 Ionization chamber correction factors for MR-linacs *Phys. Med. Biol.* **63** 11NT03
Raaijmakers A J E, Raaymakers B W and Lagendijk J J W 2008 Magnetic-field-induced dose effects in MR-guided radiotherapy systems: dependence on the magnetic field strength *Phys. Med. Biol.* **53** 909–23
Raaymakers B W *et al* 2009 Integrating a 1.5 T MRI scanner with a 6 MV accelerator: proof of concept *Phys. Med. Biol.* **54** N229–37
Raaymakers B W *et al* 2017 First patients treated with a 1.5 T MRI-linac: clinical proof of concept of a high-precision, high-field MRI guided radiotherapy treatment *Phys. Med. Biol.* **62** L41–50
Raaymakers B W, Raaijmakers A J E, Kotte A N T J, Jette D and Lagendijk J J W 2004 Integrating a MRI scanner with a 6 MV radiotherapy accelerator: dose deposition in a transverse magnetic field *Phys. Med. Biol.* **49** 4109–18
Reynolds M, Fallone B G and Rathee S 2013 Dose response of selected ion chambers in applied homogeneous transverse and longitudinal magnetic fields *Med. Phys.* **40** 042102
Smit K, van Asselen B, Kok J G M, Aalbers A H L, Lagendijk J J W and Raaymakers B W 2013 Towards reference dosimetry for the MR-linac: magnetic field correction of the ionization chamber reading *Phys. Med. Biol.* **58** 5945–57
Spindeldreier C K, Schrenk O, Bakenecker A, Kawrakow I, Burigo L, Karger C P, Greilich S and Pfaffenberger A 2017 Radiation dosimetry in magnetic fields with Farmer-type ionization chambers: determination of magnetic field correction factors for different magnetic field strengths and field orientations *Phys. Med. Biol.* **62** 6708–28
van Asselen B, Woodings S J, Hackett S L, van Soest T L, Kok J G M, Raaymakers B W and Wolthaus J W H 2018 A formalism for reference dosimetry in photon beams in the presence of a magnetic field *Phys. Med. Biol.* **63** 125008
Weinhous M S and Meli J A 1984 Determining P_{ion}, the correction factor for recombination losses in an ionization chamber *Med. Phys.* **11** 846–9
Woodings S J *et al* 2018 Beam characterisation of the 1.5 T MRI-linac *Phys. Med. Biol.* **63** 085015